Sensitivity Analysis of a Stator Current-based MRAS Estimator for Sensorless Induction Motor Drives

Mohamed S. Zaky
Department of Electrical Engineering, College of Engineering, Northern Border University, Arar, 1321, Saudi Arabia
mohamed.zaky@nbu.edu.sa (corresponding author)

Mohamed K. Metwaly
Department of Electrical Engineering, College of Engineering, Taif University, Taif, 21974, Saudi Arabia
m.metwally@tu.edu.sa

Received: 14 August 2024 | Revised: 3 September 2024 | Accepted: 8 September 2024

 DOI: https://doi.org/10.48084/etasr.8737

ABSTRACT

The sensitivity of speed estimators for parameter variations presents a significant challenge for sensorless Induction Motor (IM) drives, particularly at very low speeds. This paper examines the impact of parameter variations and the PI adaptation mechanism on the stator current-based Model Reference Adaptive System (MRAS). In contrast to the estimation of rotor flux, the MRAS method uses the observed stator current and the stator current estimate error within the adjustable IM model. The stability analysis for changes in machine parameters and PI controller gains is examined using small-signal perturbation. Additionally, a sensitivity analysis of stator and rotor resistance changes is included. A complete simulation using MATLAB/Simulink and experimental validation using a laboratory prototype based on the DSP-DS1103 are provided. The analytical, modeling, and measurement results reveal that the suggested observer responds well and provides precise speed estimation in all four quadrants of operation.

Keywords-MRAS; speed estimation; low speed; stability analysis; rotor resistance; stator resistance

I. INTRODUCTION

A variety of speed estimation techniques have recently been developed with the objective of producing high-performance speed-sensorless Induction Motor (IM) drives over an extensive range of speeds [1-5]. The Model Reference Adaptive System (MRAS) is regarded as one of the model-based approaches for speed observers in sensorless IM drives. MRAS offers several advantages, including adaptability, rapid convergence, a short computing time, and ease of integration. MRAS estimators are classified into distinct categories based on the variable they produce. The most common include rotor flux-based MRAS, back EMF-based MRAS, reactive power-based MRAS, and stator current-based MRAS [6, 7]. The presence of open integration in the Voltage Model (VM) poses challenges to starting conditions and drift in MRAS techniques that employ rotor flux as an output variable. Consequently, a low-pass filter can be employed as a substitute for pure integration; however, this results in a reduction in precision in the speed estimate at low speeds and the introduction of a time delay. Back EMF-based MRAS involves the usage of the latter as an alternative to rotor flux, which is susceptible to open integration issues. Consequently, low-pass filters, which restrict bandwidth, are not necessary as they are in the case of rotor flux-based MRAS. However, alterations to the reference model parameters, particularly those pertaining to stator resistance, may lead to inaccurate speed predictions at low speeds. In the case of a stator current-based MRAS observer, the speed estimation model employs rotor flux, which is described in terms of stator voltage, stator current, and motor characteristics [7]. This technology markedly enhances the functionality of sensorless drives at low speeds [6].

PI controllers are a commonly used adaptation mechanism for standard MRAS estimators due to their simple design and ability to provide satisfactory performance across a wide range of actions. However, given the inherent variability in machine parameters and operating circumstances, fixed-gain PI controllers may not be capable of delivering the requisite performance [8]. Recently, speed sensorless IM drives have adopted Artificial Neural Network (ANN)-based MRAS [8, 9] and Fuzzy Logic Controller-based (FLC) MRAS. In comparison to traditional mathematical model-based techniques, ANN-based methods for predicting an IM drive's parameters have proved to be more effective. In the case of a reactive power observer-based speed estimate, an FLC based

on MRAS has been employed, replacing the traditional proportional-integral (PI) adaptive mechanism with an adaptive fuzzy one. In order to minimize the speed tuning signal required for the calculation of rotor speed, a FLC has been used as a nonlinear optimizer. Authors in [10], introduce X-MRAC, a newly developed reference adaptive controller. In [11], a second-order sliding-mode current observer based on rotor flux-based MRAS is presented, along with stator resistance and parallel speed estimators. In [12], the MRAS approach was applied with two variances between electromagnetic torques and rotor fluxes. In [13], a novel formulation of reactive-power-based MRAS is proposed.

In operating circumstances at/or near zero speed, the primary issues with MRAS-based sensorless observers are their sensitivity to variations in machine parameters, faults in the acquisition of the stator voltages and currents, nonlinearity in the inverter, and pure integration of the rotor flux. The efficacy of any MRAS technique must be assessed based on its capacity to address these challenges, particularly at low and zero speeds. However, the majority of these techniques demonstrate a decline in performance as they approach or even deviate from zero speed, and the majority of these techniques have not been evaluated at zero electrical frequency [6, 14]. These factors render the development of a reliable speed estimation technique challenging in the presence of fluctuations in stator resistance. Accordingly, the principal objective of this paper is to present a novel formulation for the stator current-based MRAS speed observer, with the aim of enhancing its robustness to fluctuations in stator resistance, which have a detrimental impact on speed estimation at low and zero speeds. Moreover, to enhance the precision and resilience of the estimation to fluctuations in parameters, the proposed MRAS observer uses the observed stator current and the stator current estimation error in the adjustable model of the IM, rather than the rotor flux. This study analyzes the stability of the proposed MRAS observer in response to changes in machine parameters and PI controller gains. It presents the stability performance of the new MRAS observer using a pole-zero map, as the adaptive PI gains are varied. Furthermore, a sensitivity analysis is presented for modifications in rotor and stator resistance. To validate the proposed approach, a variety of modeling and experimental tests under different operating conditions are presented. The paper proceeds with the presentation of the dynamic model of the IM, the conventional stator current-based MRAS observer, the stability analysis and sensitivity analysis of the new stator current-based MRAS observer, as well as an examination of its stability under conditions of parameter deviation. The results of the simulations and experiments are discussed after, with regard to the various operating conditions.

II. IM DYNAMIC MODEL

Using the stator current and rotor flux, the IM dynamic model is:

$$p\vec{i}_s^s = A_{11}\vec{i}_s^s + A_{12}\vec{\lambda}_r^s + b_1\vec{v}_s^s \quad (1)$$

$$p\vec{\lambda}_r^s = A_{21}\vec{i}_s^s + A_{22}\vec{\lambda}_r^s \quad (2)$$

The electromechanical formula can be obtained using:

$$T_e = J\frac{d\omega_r}{dt} + B\omega_r + T_L \quad (3)$$

where the expression for electromagnetic torque is:

$$T_e = \frac{3}{2}\cdot\frac{p}{2}\cdot\frac{L_m}{L_r}\left[i_{qs}^s\lambda_{dr}^s - i_{ds}^s\lambda_{qr}^s\right] \quad (4)$$

where $\vec{i}_s^s = \left[i_{ds}^s \;\; i_{qs}^s\right]^T$ is the stator current vector in d-q axes, $\vec{\lambda}_r^s = \left[\lambda_{dr}^s \;\; \lambda_{qr}^s\right]^T$ is the rotor flux vector in d-q axes, $\vec{v}_s^s = \left[v_{ds}^s \;\; v_{qs}^s\right]^T$ is the stator voltage vector in d-q axes, L_m, L_s, and L_r are the magnetizing, stator, and rotor inductances, R_s and R_r are the stator and rotor resistances, T_r is the rotor time constant, ω_r and ω_{sl} are the motor and slip speeds, T_e and T_L are the developed and load torques, respectively. $A_{11} = a_1 I$, $A_{12} = a_2 I - a_3\omega_r J$, $A_{21} = a_5 I$, $A_{22} = -a_4 I - \omega_r J$, $b_1 = bI$, $a_1 = -\left(\frac{R_s}{\sigma L_s} + \frac{L_m^2}{\sigma L_s T_r L_r}\right)$, $a_2 = \frac{L_m}{\sigma L_s L_r T_r}$, $a_3 = \frac{L_m}{\sigma L_s L_r}$, $a_4 = \frac{1}{T_r}$, $a_5 = \frac{L_m}{T_r}$, $b = \frac{1}{\sigma L_s}$, $I = \begin{bmatrix}1 & 0\\ 0 & 1\end{bmatrix}$, $J = \begin{bmatrix}0 & -1\\ 1 & 0\end{bmatrix}$, $\sigma = 1 - \frac{L_m^2}{L_s L_r}$, $T_r = \frac{L_r}{R_r}$.

Figure 1 shows the block diagram for the proposed sensorless Indirect Field-Oriented Torque Control (IFOTC) of IM. In this approach, the observed speed and slip speed are employed to ascertain the unit vector, which is essential for axis transformation : $\theta_e = \int(\hat{\omega}_r + \omega_{sl})dt$.

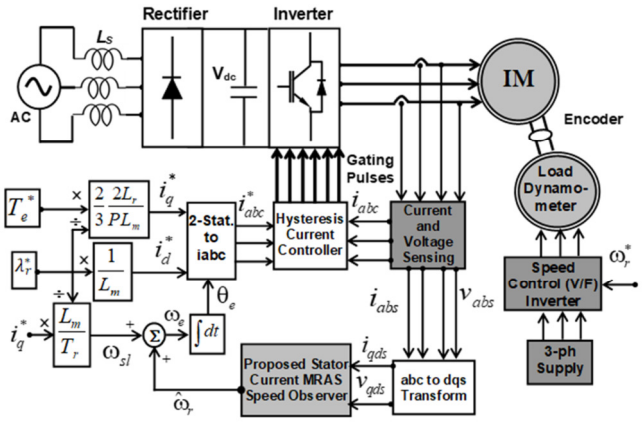

Fig. 1. Block layout of the suggested stator current-based MRAS observer for sensorless IM drive IFOTC.

In IFOC, the q-axis rotor flux is set to zero and the d-axis rotor flux is fixed. Consequently, the electromagnetic torque can be controlled exclusively by the q-axis stator current. This leads to the following:

$$\lambda_{qr}^s = 0 \quad (5)$$

$$\frac{d\lambda_{qr}^s}{dt} = 0 \quad (6)$$

$$\frac{\lambda_{dr}^s}{dt} = 0 \quad (7)$$

Then, the expression for electromagnetic torque becomes:

$$T_e = \frac{3}{2}\cdot\frac{p}{2}\cdot\frac{L_m}{L_r}\left[i_{qs}^s\lambda_{dr}^s\right] \quad (8)$$

Using (5)–(8) and substituting into (1)–(2) gives:

$$i_{dr}^{s} = 0 \quad (9)$$

$$i_{qr}^{s} = -\frac{L_m}{L_r} i_{qs}^{s} \quad (10)$$

$$\lambda_{dr}^{s} = L_m i_{ds}^{s} \quad (11)$$

$$\omega_{sl} = \frac{L_m}{T_r}\frac{i_{qs}^{s}}{\lambda_{dr}^{s}} = \frac{1}{T_r}\frac{i_{qs}^{s}}{i_{ds}^{s}} \quad (12)$$

III. STATOR CURRENT-BASED MRAS OBSERVER

The traditional stator current-based MRAS estimator for sensorless IM drive, is:

$$\lambda_{dr}^{s} = \frac{L_r}{L_m}\left[\int (v_{ds}^{s} - R_s i_{ds}^{s})dt - \sigma L_s i_{ds}^{s}\right] \quad (13)$$

$$\lambda_{qr}^{s} = \frac{L_r}{L_m}\left[\int (v_{qs}^{s} - R_s i_{qs}^{s})dt - \sigma L_s i_{qs}^{s}\right] \quad (14)$$

The stator current can be expressed using the rotor flux and motor speed as:

$$i_{ds}^{s} = \frac{1}{L_m}\left(\lambda_{dr}^{s} + \omega_r T_r \lambda_{qr}^{s} + T_r \frac{d\lambda_{dr}^{s}}{dt}\right) \quad (15)$$

$$i_{qs}^{s} = \frac{1}{L_m}\left(\lambda_{qr}^{s} - \omega_r T_r \lambda_{dr}^{s} + T_r \frac{d\lambda_{qr}^{s}}{dt}\right) \quad (16)$$

Equations (15) and (16), along with the observed speed, allow us to estimate the stator current as:

$$\hat{\imath}_{ds}^{s} = \frac{1}{L_m}\left(\lambda_{dr}^{s} + \hat{\omega}_r T_r \lambda_{qr}^{s} + T_r \frac{d\lambda_{dr}^{s}}{dt}\right) \quad (17)$$

$$\hat{\imath}_{qs}^{s} = \frac{1}{L_m}\left(\lambda_{qr}^{s} - \hat{\omega}_r T_r \lambda_{dr}^{s} + T_r \frac{d\lambda_{qr}^{s}}{dt}\right) \quad (18)$$

Note that the measured stator voltages and currents are used to determine the rotor fluxes (λ_{qr}^{s}, λ_{dr}^{s}) in (17) and (18). The stator current difference can be calculated as:

$$e_{id} = \frac{T_r}{L_m}\lambda_{qr}^{s} e_\omega \quad (19)$$

$$e_{iq} = -\frac{T_r}{L_m}\lambda_{dr}^{s} e_\omega \quad (20)$$

where, $e_{id} = (i_{ds}^{s} - \hat{\imath}_{ds}^{s})$, $e_{iq} = (i_{qs}^{s} - \hat{\imath}_{qs}^{s})$, $e_\omega = (\omega_r - \hat{\omega}_r)$. The following formula can be found by multiplying (19) and (20) by the rotor flux and adding them together:

$$e_{id}\lambda_{qr}^{s} - e_{iq}\lambda_{dr}^{s} = \frac{T_r}{L_m} e_\omega (\lambda_r^{s})^2 \quad (21)$$

where, $(\lambda_r^{s})^2 = \left(\lambda_{dr}^{s\,2} + \lambda_{qr}^{s\,2}\right)$. The speed error can be calculated and expressed using (21), as:

$$e_\omega = k\left[e_{id}\lambda_{qr}^{s} - e_{iq}\lambda_{dr}^{s}\right] \quad (22)$$

where, $k = \frac{L_m}{T_r}\frac{1}{(\lambda_r^{s})^2}$.

The conventional block diagram of the stator current-based MRAS observer is presented in Figure 2. The stator current and rotor flux are employed in the calculation of the speed estimate error, as per the specifications set forth in (22). The primary limitation of the traditional stator current-based MRAS speed observer is its tendency to provide inaccurate estimates at very low and zero speeds. It is possible to employ a VM and Current Model (CM) flux observer, as the estimation of rotor flux is a prerequisite for the implementation of the stator-current MRAS technique, as shown in (15) and (16). The rotor flux calculation was performed using the VM approach. This model provides the rotor flux components in terms of the stator current components and the rotor speed, as can be seen in (13) and (14). Any reduction in the estimated speed is fed back to the flux observer, resulting in instability in the low-speed range. This is due to the fact that the estimation of rotor flux with a CM is dependent on the estimated speed. The use of the CM flux observer to estimate speed becomes unstable when the estimation of rotor flux deteriorates, as this impacts the tracking of stator current [14].

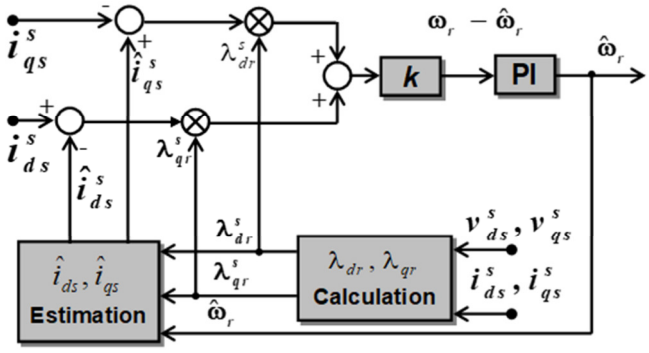

Fig. 2. The configuration of the speed estimate technique with the traditional stator current-based MRAS observer.

IV. NEW STATOR CURRENT-BASED MRAS OBSERVER

A. Speed Estimation Law

By applying this technique, the following equations are derived by multiplying (19) and (20) by the d-q components of the stator current:

$$e_{id} i_{ds}^{s} = \frac{T_r}{L_m} i_{ds}^{s} \lambda_{qr}^{s} e_\omega \quad (23)$$

$$e_{iq} i_{qs}^{s} = -\frac{T_r}{L_m} i_{qs}^{s} \lambda_{dr}^{s} e_\omega \quad (24)$$

The sum of (23) and (24) provides:

$$e_{iq} i_{qs}^{s} + e_{id} i_{ds}^{s} = -\frac{T_r}{L_m} e_\omega \left(i_{qs}^{s}\lambda_{dr}^{s} - i_{ds}^{s}\lambda_{qr}^{s}\right) \quad (25)$$

In accordance with the findings of (25), the speed error can be expressed as:

$$e_\omega = \frac{n}{T_e}\left[-e_{id} i_{ds}^{s} - e_{iq} i_{qs}^{s}\right] \quad (26)$$

where, $n = \frac{L_m}{T_r} K_{Te}$, and $K_{Te} = \frac{3}{2}\cdot\frac{p}{2}\cdot\frac{L_m}{L_r}$. Subsequently, the estimated speed is:

$$\hat{\omega}_r = k_{p\omega} e_\omega + k_{i\omega} \int e_\omega \, dt \quad (27)$$

The speed estimation error is calculated using the observed stator current and the stator current estimation error, as shown in (26). In (27), a PI controller with the optimal gains ($k_{p\omega}$ and $k_{i\omega}$) is used to consistently diminish the speed estimation error to zero. This estimation approach allows for rapid convergence and precise speed estimation, as the stator current error is

expressed as a function of the speed estimation error's first degree. It is noteworthy that (27) exhibits enhanced resilience to fluctuations in rotor and stator resistances. Additionally, the flux estimation is not employed directly in the speed computation.

B. Stability Analysis of the Modified MRAS Speed Observer

By substituting the rotor fluxes of (13) and (14) into (23) and (24), the speed estimation signal of (26), with the use of Laplace transform, is:

$$e_\omega = \frac{n}{T_e}\frac{T_r L_r}{L_m^2}\begin{bmatrix}\left\{\frac{\left(v_{ds}^s i_{ds}^s + v_{qs}^s i_{qs}^s - R_s(i_{ds}^{s\,2} + i_{ds}^{s\,2})\right)}{s}\right\} \\ -\{\sigma L_s i_{ds}^s (i_{ds}^{s\,2} + i_{ds}^{s\,2})\}\end{bmatrix}\Delta\omega_r \quad (28)$$

The MRAS observer stability to changes of the machine parameters and PI controller gains can be investigated using small-signal-perturbation analysis. Now, the variables: $i_{ds}^s = i_{dso}^s + \Delta i_{ds}^s$, $i_{qs}^s = i_{qso}^s + \Delta i_{qs}^s$, $e_\omega = e_{\omega o} + \Delta e_\omega$, and $\hat{\omega}_r = (\hat{\omega}_{r0} + \Delta\hat{\omega}_r)$. Thus, the perturbed error signal of (28) can be written as given in (29):

$$\Delta e_\omega = G(s)\Delta\hat{\omega}_r \quad (29)$$

The transfer function $G(s)$ can be expressed as:

$$G(s) = g_1 g_2 \Delta i_{ds}^s + g_1 g_3 \Delta i_{qs}^s \quad (30)$$

where, $g_1 = \frac{n}{T_e}\frac{T_r L_r}{L_m^2}$, $g_2 = \frac{1}{s}[v_{dso}^s - 2R_s i_{dso}^s - s(2\sigma L_s i_{dso}^s)]$, $g_3 = \frac{1}{s}\left[v_{qso}^s - 2R_s i_{qso}^s - s\left(2\sigma L_s i_{qso}^s\right)\right]$. The speed estimation of (27) can be expressed as:

$$\hat{\omega}_r = G(s)G_{pi}(s)\Delta\omega_r \quad (31)$$

where, $G_{pi}(s) = k_{p\omega} + \frac{k_{i\omega}}{s}$ is the transfer function of the PI controller. The closed loop transfer function of the new MRAS-based speed observer was:

$$T(s) = \frac{\hat{\omega}_r}{\omega_r} = \frac{G(s)G_{pi}(s)}{1+G(s)G_{pi}(s)} \quad (32)$$

The block diagram of a closed-loop MRAS speed observer used for the stability analysis is presented in Figure 3. In order to conduct a stability analysis, a small-signal perturbation is applied to the estimated speed. Assuming that the actual motor speed (ω_r) is constant, it is determined that both the variation of ω_r and $\Delta\omega_r$ are equal to zero. The estimated speed is subjected to a perturbation, $\Delta\hat{\omega}_r$. If the system is stable, then the variation in the estimated speed, $\Delta\hat{\omega}_r$, will diminish over time, allowing the estimated speed to revert to its previous stable state. Therefore, according to Fig. 3, $\omega_r = \hat{\omega}_{r0}$ as $\omega_r - \hat{\omega}_r = \omega_r - (\hat{\omega}_{r0} + \Delta\hat{\omega}_r) = -\Delta\hat{\omega}_r$ at the stable operating point around which the system is perturbed. The closed-loop transfer function of MRAS observer is derived as described in (33):

$$T(s) = \begin{matrix}\frac{(g_4-1)s^2+g_5 s+g_6}{g_4 s^2+g_5 s+g_6}\Delta i_{ds}^s + \\ \frac{(g_7-1)s^2+g_8 s+g_9}{g_7 s^2+g_8 s+g_9}\Delta i_{qs}^s\end{matrix} \quad (33)$$

where, $g_4 = \left[1 - 2g_1\sigma L_s i_{dso}^s k_{p\omega}\right]$, $g_5 = \left[g_1 v_{dso}^s k_{p\omega} - 2g_1 R_s i_{dso}^s k_{p\omega} - 2g_1\sigma L_s i_{dso}^s k_{i\omega}\right]$, $g_6 = [g_1 v_{dso}^s k_{i\omega} - 2g_1 R_s i_{dso}^s k_{i\omega}]$, $g_7 = \left[1 - 2g_1\sigma L_s i_{qso}^s k_{p\omega}\right]$, $g_8 = \left[g_1 v_{qso}^s k_{p\omega} - 2g_1 R_s i_{qso}^s k_{p\omega} - 2g_1\sigma L_s i_{qso}^s k_{i\omega}\right]$, $g_9 = \left[g_1 v_{qso}^s k_{i\omega} - 2g_1 R_s i_{qso}^s k_{i\omega}\right]$.

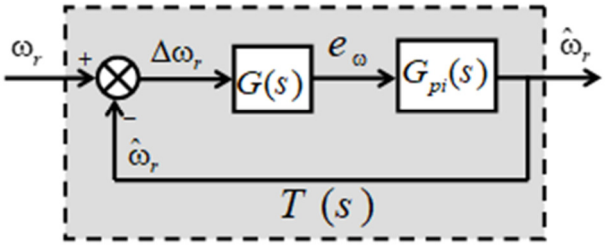

Fig. 3. Block diagram of closed-loop new MRAS speed observer used for stability analysis.

As shown in (33), the transfer function *T(s)* of the novel MRAS speed observer is contingent upon the IM parameters and the PI controller gains ($k_{p\omega}$, $k_{i\omega}$). Figure 4(a) shows the stability performance of the new MRAS observer using a pole-zero map in response to changes in the $k_{i\omega}$ parameter (ranging from 0.1 to 1000). While the MRAS observer is stable with respect to variations in $k_{i\omega}$, its stability is compromised when $k_{i\omega}$ is low (0.1 to 100), resulting in a decline in performance. This suggests that the variation of $k_{i\omega}$ has a significant impact on the stability of the MRAS. The pole-zero map of the MRAS observer was also examined for $k_{p\omega}$ variations (0.1 to 1000), as presented in Figure 4(b). It was observed that $k_{p\omega}$ variations in the range (0.1 to50) resulted in a good performance and stability of the MRAS observer. Further increases, led to the dominant pole and zero moving towards the imaginary axis, resulting in a deterioration in stability.

C. Robustness to Parameter Variation

In order to analyze the new MRAS performance and stability, the frequency response is employed, as the phase margin provides an appropriate measure of the MRAS stability margin. This study examines the performance of the novel MRAS observer in terms of the Phase Margin (PM) when subjected to variations in R_s and R_r, as presented in the results shown in Figure 5. As previously stated, the proposed new MRAS exhibits minimal alteration in response to variations in R_s and R_r. Despite the impact of R_s and R_r on the PM, the system remains stable, with a PM that is high and well above the critical stability limit. It is evident that the proposed new MRAS observer exhibits high performance and robust stability in the presence of variations in machine parameters.

V. EXPERIMENTAL SETUP

The proposed sensorless IM drive, which employs a novel stator current-based MRAS observer with PI in the adaptation mechanism, was subjected to experimental implementation in real-time using a dSPACE DSP-DS1103 control board for a laboratory 5.5 kW IM, as shown in Figure 6. The machine under test was operated in a sensorless torque-controlled mode. The speed of the drive is controlled by the speed-controlled load dynamometer. The IM is supplied with a three-phase

voltage-source pulse width modulation (PWM) inverter, comprising six IGBTs and a gate driver board.

(a)

(b)

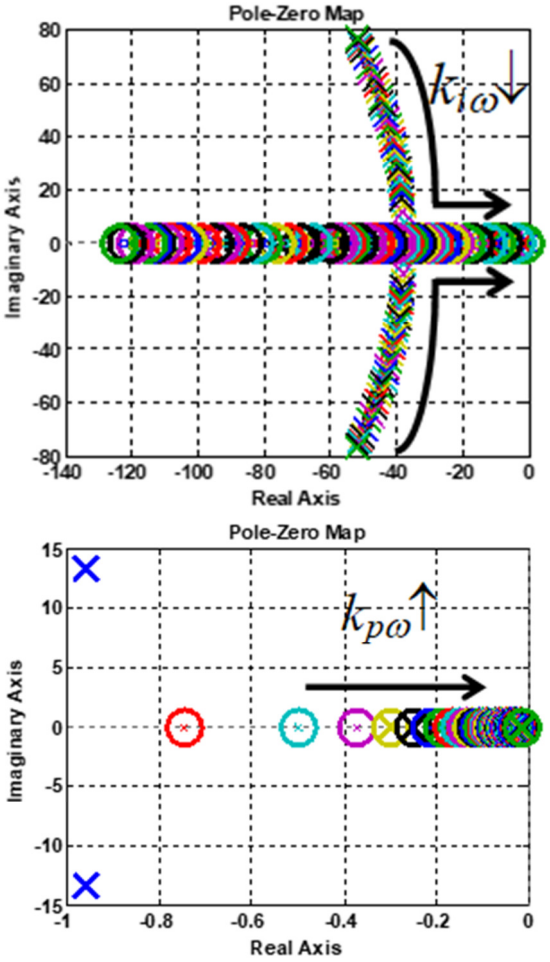

Fig. 4. Stability performance of the new MRAS observer using Pole-Zero Map under variation of the adaptive PI gains, (a) change of $k_{i\omega}$, and (b) change of $k_{p\omega}$. (zooming in the dominant poles and zeros locations).

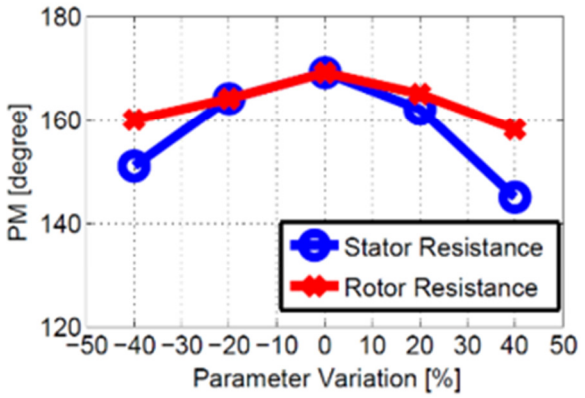

Fig. 5. Stability performance of the new MRAS observer in frequency domain under R_s and R_r variations.

To validate the simulation outcomes and demonstrate the efficacy of the proposed observer with PI in the adaptation mechanism, the experimental results are presented under identical conditions to those of the simulation for a fair comparison of performance. The results were obtained under IFOTC of the sensorless IM drive. In the experimental results, the IM was operated under torque control with standard dq current loops, and the estimated flux angle was employed for vector transformation of the rotor-oriented dq frame. The IM drive system was connected to a speed-controlled load dynamometer, the speed of which was monitored. In this IFOC of a sensorless IM drive, the reference d-axis current is calculated using the rotor flux constant value (11). To calculate the slip speed (12) is used. The unit vector is calculated and employed in the transformation of the d-axis and q-axis reference currents to the abc reference currents. The PWM signals of the gate driver circuit to drive the six IGBTs are generated by comparing the reference and measured abc currents.

VI. SIMULATION AND EXPERIMENTAL RESULTS

In order to validate the effectiveness of the proposed new MRAS speed observer for use in a sensorless IM drive, a simulation model has been constructed using Matlab/Simulink. The parameters of the IM used for simulation and experimental verification are presented in Table I. In both the simulation and experimental results, the sensorless IM was operated under torque control with standard dq current loops. All figures are divided into six subfigures for the purposes of clarity and ease of reference. The figure shows the actual (black) and estimated (red) speeds. The discrepancy between the actual and estimated speeds is outlined also. Additionally, the current in quadrature, iq, in per unit value is presented, together with the stator currents in the αβ frame. Furthermore, the reference (black) and estimated (red) rotor flux angles in electrical degrees (deg) is shown, with the deviation of the reference and estimated flux angles. Figure 7 shows the simulation and experimental results of the sensorless IM drive during sudden application and removal of the rated load torque at a speed of 20 rpm. The results of the simulation and experiment demonstrate the performance of the sensorless IM drive during reversals at very low speeds, ±20 rpm, at the rated load. These results are presented in Figure 8. It is observed that the proposed MRAS observer demonstrates a notable performance with exceptional estimation accuracy during very low-speed reversals.

TABLE I. PARAMETERS OF IM

Rated power	**5.5 kW**	L_s	**57.3 mH**
No. of pole pairs (P)	2	L_r	57.3 mH
Stator resistance (R_s)	0.294 Ω	L_m	56.43 mH
Rotor resistance (R_r)	0.14325 Ω	Rated voltage	186 V
		Supply frequency	50 Hz

VII. CONCLUSIONS

This paper proposes a modified stator current-based Model Reference Adaptive System (MRAS) speed observer. The sensorless Induction Motor (IM) drive using the suggested MRAS observer was found to exhibit consistent performance across all four quadrants throughout the course of operation.

The sensitivity study of the estimated speed to stator and rotor resistance changes revealed that the proposed MRAS observer demonstrated minimal sensitivity to stator and rotor resistance mismatches at both high and low stator frequencies.

The gains of the PI adaptation mechanism are based on the speed estimator transfer function. Stability performance of the new MRAS observer using a pole-zero map under PI gains variation is introduced. It is evident that low values of $k_{i\omega}$ have a significant impact on the stability of the MRAS. Nevertheless, optimal performance and stability of the MRAS observer are contingent upon the gain $k_{p\omega}$ falling within the range (0.1 to 50). Further increases in this gain result in the dominant pole and zero being shifted towards the imaginary axis, thereby impairing stability. The sensorless IM drive is capable of performing effectively at extremely low speeds, including at zero electrical frequency. The efficacy of the proposed stator current-based MRAS observer is demonstrated by the results of the stability and sensitivity analysis, as well as the modeling and experimental data. In operating circumstances at extremely low and zero speeds, the proposed observer addresses the primary issues with conventional MRAS-based rotor flux and back emf, including sensitivity to parameter variation and pure integration of the rotor flux. Furthermore, it addresses the deterioration of conventional techniques as they approach zero speed or even exceed it at a gradual rate.

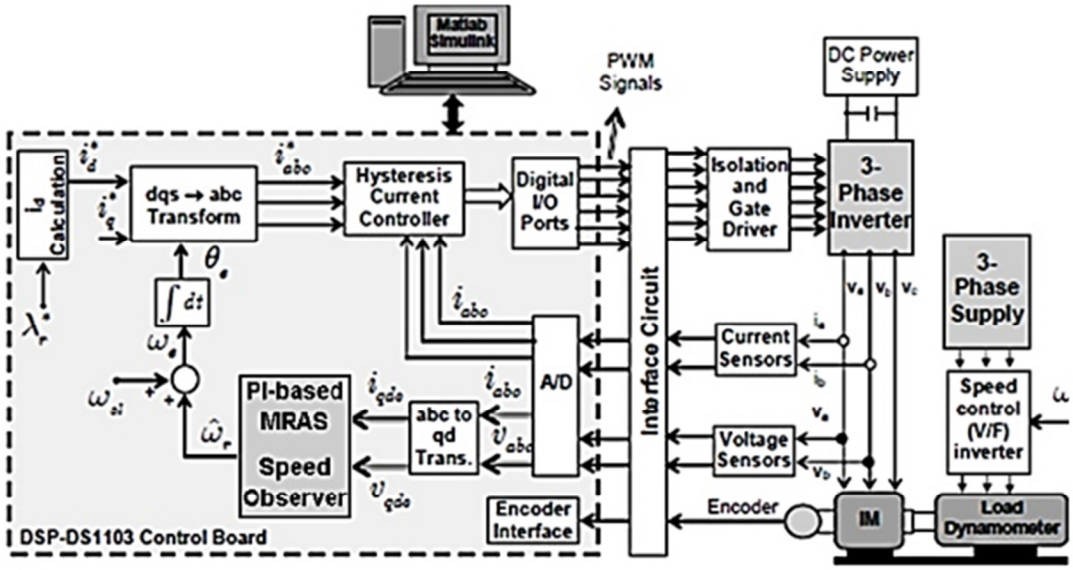

Fig. 6. Schematic diagram of the experimental system for sensorless IFOTC of an IM drive using DSP-DS1103 control board.

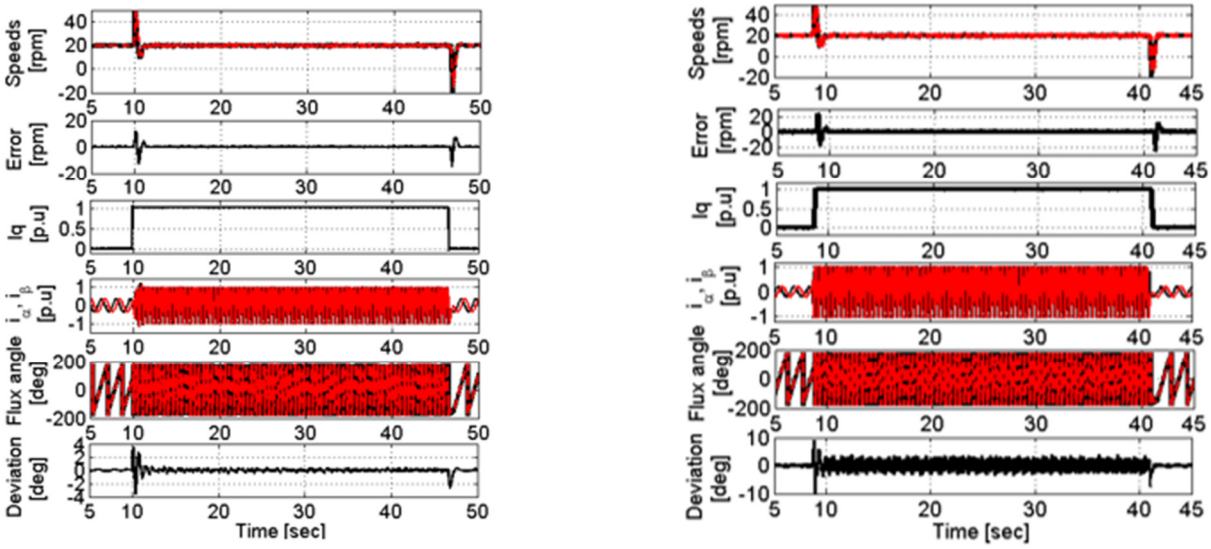

Fig. 7. Simulation (a) and experimental (b) results of the sensorless IM drive during sudden application and removal of the rated load torque at speed of 20 rpm.

(a)

(b)

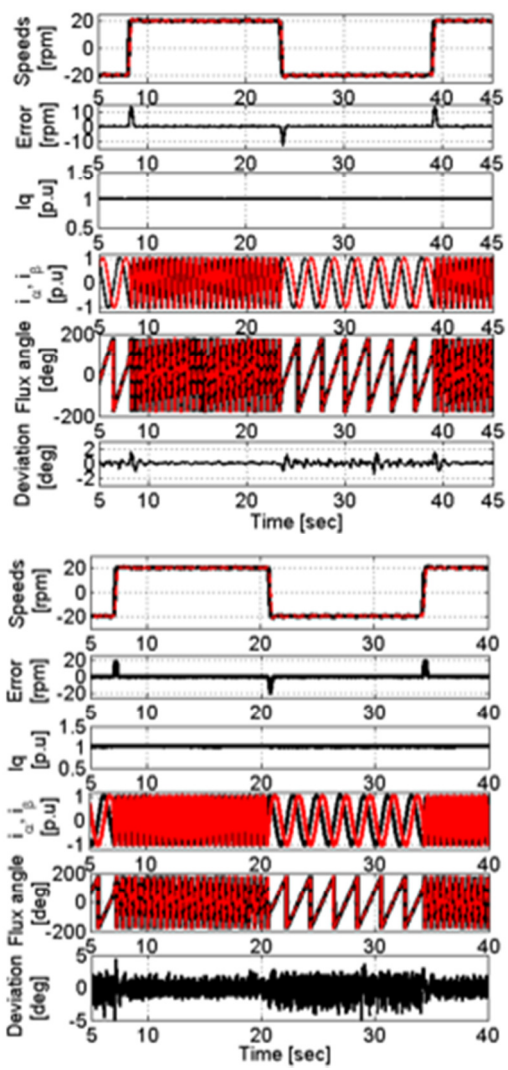

Fig. 8. Simulation (a) and experimental (b) results of the sensorless IM drive at very low speed reversal ±20 rpm at rated load.

ACKNOWLEDGMENT

The authors extend their appreciation to the Deanship of Scientific Research at Northern Border University, Arar, KSA for funding this research work through the project number "NBU-FFR-2024-1250-04."

REFERENCES

[1] M. S. Zaky, S. M. Shaaban, T. Fetouh, H. Z. Azazi, and Y. I. Mesalam, "Optimization of Observer Feedback Gains for Stable Sensorless IM Drives at Very Low Frequencies: A Comparative Study between GA and PSO," *Mathematics*, vol. 10, no. 10, Jan. 2022, Art. no. 1710, https://doi.org/10.3390/math10101710.

[2] S. Usha *et al.*, "Performance enhancement of sensorless induction motor drive using modified direct torque control techniques for traction application," *Alexandria Engineering Journal*, vol. 108, pp. 518–538, Dec. 2024, https://doi.org/10.1016/j.aej.2024.07.095.

[3] M. S. Zaky, H. A. Maksoud, and H. Z. Azazi, "Sensorless Induction Motor Drives Using Adaptive Flux Observer at Low Frequencies," *Engineering, Technology & Applied Science Research*, vol. 8, no. 1, pp. 2572–2576, Feb. 2018, https://doi.org/10.48084/etasr.1752.

[4] W. Sun, W. Zhenyu, D. Xu, and B. Wang, "Robust Stability Improvement for Speed Sensorless Induction Motor Drive at Low Speed Range by Virtual Voltage Injection," *IEEE Transactions on Industrial Electronics*, vol. 67, no. 4, pp. 2642–2654, Apr. 2020, https://doi.org/10.1109/TIE.2019.2910039.

[5] M. Zaky, T. Fetouh, S. M. Shaaban, and H. Azazi, "A Novel Analytical Approach Using Rough Set and Genetic Algorithm of a Stable Sensorless Induction Motor Drives in the Regenerating Mode," *IEEE Access*, vol. 8, pp. 157748–157761, Aug. 2020, https://doi.org/10.1109/ACCESS.2020.3019180.

[6] R. Kumar, S. Das, P. Syam, and A. K. Chattopadhyay, "Review on model reference adaptive system for sensorless vector control of induction motor drives," *IET Electric Power Applications*, vol. 9, no. 7, pp. 496–511, 2015, https://doi.org/10.1049/iet-epa.2014.0220.

[7] S. M. Gadoue, D. Giaouris, and J. W. Finch, "Stator current model reference adaptive systems speed estimator for regenerating-mode low-speed operation of sensorless induction motor drives," *IET Electric Power Applications*, vol. 7, no. 7, pp. 597–606, Aug. 2013, https://doi.org/10.1049/iet-epa.2013.0091.

[8] S. Maiti, V. Verma, C. Chakraborty, and Y. Hori, "An Adaptive Speed Sensorless Induction Motor Drive With Artificial Neural Network for Stability Enhancement," *IEEE Transactions on Industrial Informatics*, vol. 8, no. 4, pp. 757–766, Nov. 2012, https://doi.org/10.1109/TII.2012.2210229.

[9] A. Accetta, M. Cirrincione, M. Pucci, and G. Vitale, "MRAS speed observer for high performance linear induction motor drives based on linear neural networks," in *2011 IEEE Energy Conversion Congress and Exposition*, Phoenix, AZ, USA, Sep. 2011, https://doi.org/10.1109/ECCE.2011.6063997.

[10] R. Teja, C. Chakraborty, S. Maiti, and Y. Hori, "A New Model Reference Adaptive Controller for Four Quadrant Vector Controlled Induction Motor Drives," *IEEE Transactions on Industrial Electronics*, vol. 59, pp. 3757–3767, Oct. 2012, https://doi.org/10.1109/TIE.2011.2164769.

[11] L. Zhao, J. Huang, H. Liu, B. Li, and W. Kong, "Second-Order Sliding-Mode Observer With Online Parameter Identification for Sensorless Induction Motor Drives," *IEEE Transactions on Industrial Electronics*, vol. 61, no. 10, pp. 5280–5289, Oct. 2014, https://doi.org/10.1109/TIE.2014.2301730.

[12] I. Benlaloui, S. Drid, L. Chrifi-Alaoui, and M. Ouriagli, "Implementation of a New MRAS Speed Sensorless Vector Control of Induction Machine," *IEEE Transactions on Energy Conversion*, vol. 30, no. 2, pp. 588–595, Jun. 2015, https://doi.org/10.1109/TEC.2014.2366473.

[13] R. Teja, V. Verma, and C. Chakraborty, "A New Formulation of Reactive Power Based Model Reference Adaptive System for Sensorless Induction Motor Drive," *IEEE Transactions on Industrial Electronics*, vol. 62, no. 11, pp. 6797–6808, Nov. 2015, https://doi.org/10.1109/TIE.2015.2432105.

[14] Z. Tir, T. Orlowska-Kowalska, H. Ahmed, and A. Houari, "Adaptive High Gain Observer Based MRAS for Sensorless Induction Motor Drives," *IEEE Transactions on Industrial Electronics*, vol. 71, no. 1, pp. 271–281, Feb. 2023, https://doi.org/10.1109/TIE.2023.3243271.